IEEE Access
Multidisciplinary ⋮ Rapid Review ⋮ Open Access Journal

Received 21 December 2024, accepted 5 January 2025, date of publication 10 February 2025, date of current version 28 March 2025.

Digital Object Identifier 10.1109/ACCESS.2025.3540166

RESEARCH ARTICLE

The Integrated Adaptive Fault Tolerant Control Design With Saturation for Nonlinear System

CONG LIU
Aviation Maintenance NCO Academy, Air Force Engineering University, Xinyang 464000, China
e-mail: 598832156@qq.com

ABSTRACT A integrated fault tolerant control design with adaptive fault estimation algorithm is proposed in this paper, which is used for the nonlinear system with saturation. Firstly, the fault model with actuator and sensor faults is built for the nonlinear system with saturation, to simplify the controller design procedure, taking the output tracking error as the augmented state, and the extended system model is obtained. Secondly, the fault tolerant control with adaptive estimation law is proposed, in order to solve the constraints caused by saturation in the controller design, the design algorithm through convex group description is presented, meanwhile, the robust control index is introduced in the controller design, and the controller calculating principle is given through linear matrix inequality(LMI). Finally, a flight numerical example is proposed to demonstrate the effectiveness of the method presented in this paper.

INDEX TERMS Fault tolerant control, adaptive, integrated, saturation, LMI.

I. INTRODUCTION

The saturation is common in the actual system, which is the common nonlinear feature in the field of engineering control system, for example, the deflection Angle of airplane rudder is limited in the fixed amplitude. If the characteristic of actuator saturation is ignored in the controller design, which may bring declination of system, and even make the system instability and cause serious results. For example, if the saturation of actuator angle is ignored in the flight control design, the airplane may deviate from the scheduled flight trajectory and can not be controlled. Especially, the saturation should be considered in the fault tolerant control design, the main reason is that, the actuator will reach the saturation under fault in advance, for example, when the structure damage occur in the actuator, the deflection angle will reach to the saturation region in advance, if no measures is taken, the airplane will be out of control, and cause flight accident. So the research of fault tolerant control with actuator saturation is very important in the theoretical and practical field.

There are lots of research results on the fault tolerant control with actuator saturation [1], [2], [3], [4], [5], [6]. The measures to the saturation contains two aspects in common. one is that the saturation constraint is not considered when designing the controller first, and then the compensator is added in the controller to maintain the control performance. The other is that the saturation constraint is considered in the controller design, some measures are taken to make the control input in the saturation range, and this will make the actuator avoid saturation. The advantage of the first method is that when the actuator is out of saturation, the control performance can be maintained, and the saturation occur, the loss of performance can be cut down, the disadvantage of this method the compensator can not change the control performance of saturation, the system will be unstable. The advantage of second method is that the characteristics of saturation will not affect the control performance, and provide more space for controller design, of course there are disadvantages as well, it is that the solved region of controller is smaller, and can not guarantee the existence of controller, so this method has certain conservatism. In comparison, the second method has been more extensive, the reason is that the spirit of compensation is to make the actuator avoid saturation, so in this paper the second method of dealing with saturation is adopted, which will be used in the designing the fault tolerant control.

According to the different strategy of fault tolerant control, the fault control strategy with saturation can be divided into

The associate editor coordinating the review of this manuscript and approving it for publication was Jinquan Xu.

two types, one is called as active fault tolerant control, and the other is passive fault tolerant control. Compare with passive fault tolerant control strategy [7], [8], the active fault tolerant control has been applied more widely [9], [10], because the fault information can be obtained on time, and it can be used to deal with more faults types. Considering the active fault tolerant strategy, the author has presented some paper about the fault tolerant algorithms with sliding mode observer [11], [12], [13], [14], but these algorithms are not suitable for the nonlinear system with saturation, the main reasons are follows. On one hand, the saturation may break the existence condition of fault diagnosis observer, so the observer of saturated nonlinear system is hard to design, On the other hand, the input of fault tolerant control contain the fault diagnosis item, and this will make the actuator reach the saturated region, thus the satisfied control performance can not be realized. In this paper, the fault estimation scheme combined with adaptive law is proposed, and the integrated fault tolerant algorithm is presented with adaptive law.

Besides, some new control methods are absorbed in the fault tolerant control design, such as predictive control [15], [16], [17], [18], [19], [20], iterative learning control [21], [22], [23], [24], robust control [25], [26]. Huiyuan Shi etal [15] provides a robust constrained model predictive fault-tolerant control algorithm for a class of industrial processes with uncertainties, interval time-varying delay, unknown disturbances and partial actuator failures, the control gain is given through linear matrix inequalities, and satisfied fault tolerant control results can be obtained through simulation results. Paper [20] proposes a linear quadratic predictive fault-tolerant control (LQPFTC) scheme for multi-phase batch processes with input time-delay and actuator faults, and the tracking control results is realized. Limin Wang etal [23] proposes a new stochastic composite iterative learning control for batch processes with actuator faults that happen with a certain kind of probability, and the stability results of the control system is provided through LMI conditions. Through analyzing the existing results, we can find, when multiple faults occur in the system simultaneously, if the methods proposed in the previous are used for fault tolerant control, the fault estimation results will be inaccurate, or the system outputs will not maintain stable, so these methods are not suitable.

Motivated by the above discussion, in this paper, the integrated fault tolerant control algorithm is proposed for the nonlinear system with unknown disturbances, where the actuator and sensor faults are considered simultaneously. Firstly, the auxiliary state vector is introduced, and the original system are transformed into the nonlinear system with only actuator faults and unknown disturbances. Then the convex composed items are used to described the saturated actuator control input, and the adaptive mapping item with convex composed items is proposed to estimate the unknown fault. Thirdly, the fault tolerant control input with adaptive item is presented, and the calculated algorithm for controller gain is put forward through convex optimization method and linear matrix inequality technique. Finally, a flight control example are provided to illustrate the effectiveness of the algorithm proposed in this paper. The main contributions of the present work are as follows, (1) The actuator saturation is considered in the fault tolerant control design, and the convex composed method is proposed to deal with the saturation, (2) Actuator and sensor faults are considered in the nonlinear system with unknown disturbances, and the adaptive algorithm with mapping item is added in the controller, (3) the linear matrix inequality is provided to make the controller gain exist under optimization problems. Comparing the idea proposed in this paper with others, the main differences contain two points, the convex groups description is introduced to explain saturation, besides, multiple faults are considered in the fault tolerant controller design, the extended system and linear matrix inequalities are absorbed in the controller design.

The rest of the paper is organized as follows. Problems formulation is given in Section II, some assumptions and preliminaries for the nonlinear system with saturation are given in advanced. In Section III, the integrated active fault tolerant control algorithm is proposed for nonlinear system with multiple faults and disturbances. Section IV provides the calculated algorithm for the fault tolerant control gain. An example is illustrated to demonstrate the effectiveness of the proposed method in Section V. Section VI summarizes the whole paper and some conclusions can be gotten. Throughout this paper, $\boldsymbol{R}$ denotes the set of real numbers; the vector norm $\|\alpha\|$ is defined as $\|\alpha\| = \sqrt{\alpha^T \alpha}$, where α is a column vector.; for any matrix $\boldsymbol{A}$, $\|\boldsymbol{A}\|$ denotes the 2-norm $\sqrt{\lambda_{\max}(\boldsymbol{A}^T A)}$, $\lambda_{\max}(\boldsymbol{A})$ denotes the maximum eigenvalue of a matrix $\boldsymbol{A}$.

II. PROBLEM FORMULATION AND PRELIMINARIES

Consider a class of uncertain nonlinear system with multiple faults, actuator saturated constraints and disturbances, are described by the following equations,

$$\begin{cases} \dot{\boldsymbol{x}} = \boldsymbol{A}\boldsymbol{x} + \boldsymbol{g}(\boldsymbol{x}, t) + \boldsymbol{B}\boldsymbol{K}sat(\boldsymbol{u}) + \boldsymbol{F}\xi(t) \\ \boldsymbol{y} = \boldsymbol{C}\boldsymbol{x} + \boldsymbol{D}\boldsymbol{f}_s(t) \end{cases} \tag{1}$$

where $\boldsymbol{x} \in \boldsymbol{R}^n$, $\boldsymbol{u} \in \boldsymbol{R}^m$, $\boldsymbol{y} \in \boldsymbol{R}^p$ denote the state variables, control inputs, and measured outputs. $\boldsymbol{g}(\boldsymbol{x}, t)$ is local *Lipschitz* nonlinear term, and satisfies the constraint $\|\boldsymbol{g}(\boldsymbol{x}_1, t) - \boldsymbol{g}(\boldsymbol{x}_2, t)\| \le \delta \|\boldsymbol{x}_1 - \boldsymbol{x}_2\|$, $\forall t$,where δ is *Lipschitz* positive real scalar. $sat(\boldsymbol{u})$ stand for the actuator saturation function, and the detailed function is expressed as $sat(\boldsymbol{u}) = [sat(\boldsymbol{u}_1), sat(\boldsymbol{u}_2), \ldots, sat(\boldsymbol{u}_m)]^T$, where $sat(\boldsymbol{u}_i)$ satisfies $sat(\boldsymbol{u}_i) = sgn(\boldsymbol{u}_i) \cdot min\{\sigma_i, |\boldsymbol{u}_i|\}$, and σ_i represent the upper bound of actuator saturation. The matrix $\boldsymbol{K}$ can be expressed as $\boldsymbol{K} = diag\{K_1, \ldots, K_m\}$, K_i stands for the control efficiency factor of actuator, and it satisfies the inequality $0 \le K_i \le 1$. When the coefficient K_i satisfies the following equation $K_i = 0$, and this means that the ith actuator is absolutely useless. When the coefficient K_i satisfies the following equation $0 < K_i < 1$, and this means that ith actuator is partly useless, meanwhile the coefficient K_i satisfy the inequality $K_{i1} \le K_i \le K_{i2}$, and that means that the coefficient K_i is bounded, the value of upper bound is K_{i2} while the value of lower bound is K_{i1}. When the coefficient K_i satisfies the following equation $K_i = 1$, and this means that ith actuator is normal. In this paper, the case that actuator is partly useless is considered, and this means that the coefficient K_i satisfies the formula $0 < K_i < 1$. $\boldsymbol{\xi}(t)$ stands for bounded disturbances. $\boldsymbol{f}_s(t)$ means sensor faults.

Remark 1: In the actual engineering system, the actuator and sensor faults exists, and the actuator will emerge saturation, for example, in the flight control system, the actuators and angular velocity sensor will break down, and the actuator often operate in the limited amplitude. The sensor fault can be described as the additional factor $\boldsymbol{f}_s(t)$, and the actuator fault can be described as the factor $\boldsymbol{K}$. Besides, the nonlinearities and disturbances are always contained in the actual system, and they can be expressed as the item $\boldsymbol{g}(\boldsymbol{x}, t)$ and $\xi(t)$. So the nonlinear system proposed in this paper can be described as Eq.1.

Remark 2: The upper bound K_{i2} can be chosen as one, if the value K_{i2} is greater than one, through the normalization processing, the formula $|K_{i2}| < 1$ is right.

Remark 3: The nonlinear term $\boldsymbol{g}(\boldsymbol{x}, t)$ satisfies local *Lipschitz* condition, in the actual engineering system, the global *Lipschitz* condition can not be satisfied easily, but by the dealing of linearization or mathematical transforming, the local *Lipschitz* condition can be realized easily.

For the nonlinear system with multiple faults shown in the formula (1), considering the constraints that the actuator is restricted by saturation, in order to obtain the suitable control performance of tracking, the controller algorithm is designed as the following program. First the extended system is built according to the given tracking control objective and original system, and the original system with multiple faults can be transformed into the extended system with actuator fault. Then the convex group method is introduced to tackle the saturation, this measure can make sure the actuator will work in the bound and avoid saturation. Finally the adaptive estimate item related to the actuator fault is combined in the fault tolerant control, and the linear matrix inequalities are used to obtain the calculated algorithm for the controller. The fault tolerant control design block is shown in Fig1, and the flow chart of proposed method in this paper is shown in Fig2.

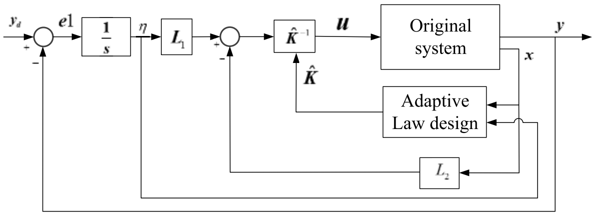

FIGURE 1. The design program of controller.

In Figure 1, $\boldsymbol{y}_d$ stands for the given control objective. $\boldsymbol{L}$ denote the gain matrix of controller, and it can be expressed as $\boldsymbol{L} = \begin{bmatrix} \boldsymbol{L}_1 & -\boldsymbol{L}_2 \end{bmatrix}$. $\hat{\boldsymbol{K}}$ is the designed control law for estimating the actuator faults. The objective of fault tolerant control design is that the output $\boldsymbol{y}$ can reach the given value $\boldsymbol{y}_d$ under multiple faults. In figure2, the whole flow chart of proposed controller is shown, and the fault tolerance control input is described in the figure.

Pay attention to the block shown in Figure1, the fault diagnosis item is not contained in the controller design obviously, but contained in the adaptive law design, so the fault diagnosis and fault tolerant control are combined together, and the integrated controller algorithm is provided.

III. THE INTEGRATED ACTIVE FAULT TOLERANT CONTROL DESIGN COMBINING ADAPTIVE ESTIMATED ALGORITHM

According to the nonlinear system shown as (1), define $\boldsymbol{\eta}$ as the following formula $\boldsymbol{\eta} = \int_0^t \left(\boldsymbol{y}_d(\tau) - \boldsymbol{y}(\tau)\right) d\tau$, and the $\boldsymbol{e}1$ stands for $\boldsymbol{e}1 = \boldsymbol{y}_d - \boldsymbol{y}$, then the derivative of $\boldsymbol{\eta}$ can be expressed as $\dot{\boldsymbol{\eta}} = \boldsymbol{y}_d - \boldsymbol{Cx} - \boldsymbol{Df}_s(t)$. Under these conditions, the integrated active fault tolerant controller is shown as formula(2), and the controller is designed on the state and output vector,

$$\boldsymbol{u} = \hat{\boldsymbol{K}}^{-1}\boldsymbol{L}_1\boldsymbol{\eta} - \hat{\boldsymbol{K}}^{-1}\boldsymbol{L}_2\boldsymbol{x} \tag{2}$$

where $\boldsymbol{L}_1, \boldsymbol{L}_2$ are the designed gain matrix, $\hat{\boldsymbol{K}}$ stands for the actuator estimation, the detailed design algorithm will be provided later. As the estimates $\hat{\boldsymbol{K}}$ is contained in control input $\boldsymbol{u}$, so the controller can be called as integrated active fault tolerant controller. In addition, define new vector $\boldsymbol{\varsigma}$ and $\boldsymbol{L}$, and the detailed information are shown as $\boldsymbol{\varsigma} = \begin{bmatrix} \boldsymbol{x}^T & \boldsymbol{\eta}^T \end{bmatrix}^T$ and $\boldsymbol{L} = \begin{bmatrix} \boldsymbol{L}_1 & -\boldsymbol{L}_2 \end{bmatrix}$. Under this description, combining the formula shown in formula (1) and (2), the original system can be transformed to the following extended system shown in formula(3),

$$\dot{\boldsymbol{\varsigma}} = \bar{\boldsymbol{A}}\boldsymbol{\varsigma} + \bar{\boldsymbol{B}}\boldsymbol{K}sat\left[\hat{\boldsymbol{K}}^{-1}\boldsymbol{L}\boldsymbol{\varsigma}\right] + \boldsymbol{G}(\boldsymbol{W}\boldsymbol{\varsigma}, t) + \bar{\boldsymbol{F}}\boldsymbol{d}(t) \tag{3}$$

where $\bar{\boldsymbol{A}} = \begin{bmatrix} \boldsymbol{A} & \boldsymbol{0} \\ -\boldsymbol{C} & \boldsymbol{0} \end{bmatrix}$;$\bar{\boldsymbol{B}} = \begin{bmatrix} \boldsymbol{B} \\ 0 \end{bmatrix}$;$\boldsymbol{G}(\boldsymbol{W}\boldsymbol{\varsigma}, t) = \begin{bmatrix} \boldsymbol{g}(\boldsymbol{x}, t) \\ \boldsymbol{0} \end{bmatrix}$, $\boldsymbol{W} = \begin{bmatrix} \boldsymbol{I} & \boldsymbol{0} \end{bmatrix}$. As the item of $\boldsymbol{g}(\boldsymbol{x}, t)$ is the *Lipschitz* nonlinearity, so the nonlinear item $\boldsymbol{G}(\boldsymbol{W}\boldsymbol{\varsigma}, t)$ contains is also the *Lipschitz* nonlinearity, and it satisfies the inequality $\|\boldsymbol{G}(\boldsymbol{W}\boldsymbol{\varsigma}, t)\| \leq \psi_g \|\boldsymbol{\varsigma}\|$, where Ψ_g is the *Lipschitz* constant, $\bar{\boldsymbol{F}} = \begin{bmatrix} \boldsymbol{F} & \boldsymbol{0} & \boldsymbol{0} \\ \boldsymbol{0} & \boldsymbol{I} & -\boldsymbol{D} \end{bmatrix}$, $\boldsymbol{d}(t) = \begin{bmatrix} \boldsymbol{\xi}(t) \\ \boldsymbol{y}_d \\ \boldsymbol{f}_s(t) \end{bmatrix}$.

The control objective is that the output vector $\boldsymbol{y}_d$ can track the command output $\boldsymbol{y}_d$, under the design of control input matrix $\boldsymbol{L}_1$ and $\boldsymbol{L}_2$, the adaptive law $\hat{\boldsymbol{K}}$. The adaptive term $\hat{\boldsymbol{K}}$ is designed to estimate the actuator faults $\boldsymbol{K}$,considering the value of $\boldsymbol{K}$ is bounded, so the project law is absorbed for the adaptive term design, the detailed design procedure of $\hat{\boldsymbol{K}}$ is shown in the following.

Considering the saturation of actuator, combining the conclusion proposed in paper [27], the linear convex group is absorbed to describe the saturated nonlinearity *sat* $(\boldsymbol{u})$, which is convenient for fault tolerant control design. Based on this, we first give the definition of convex group description.

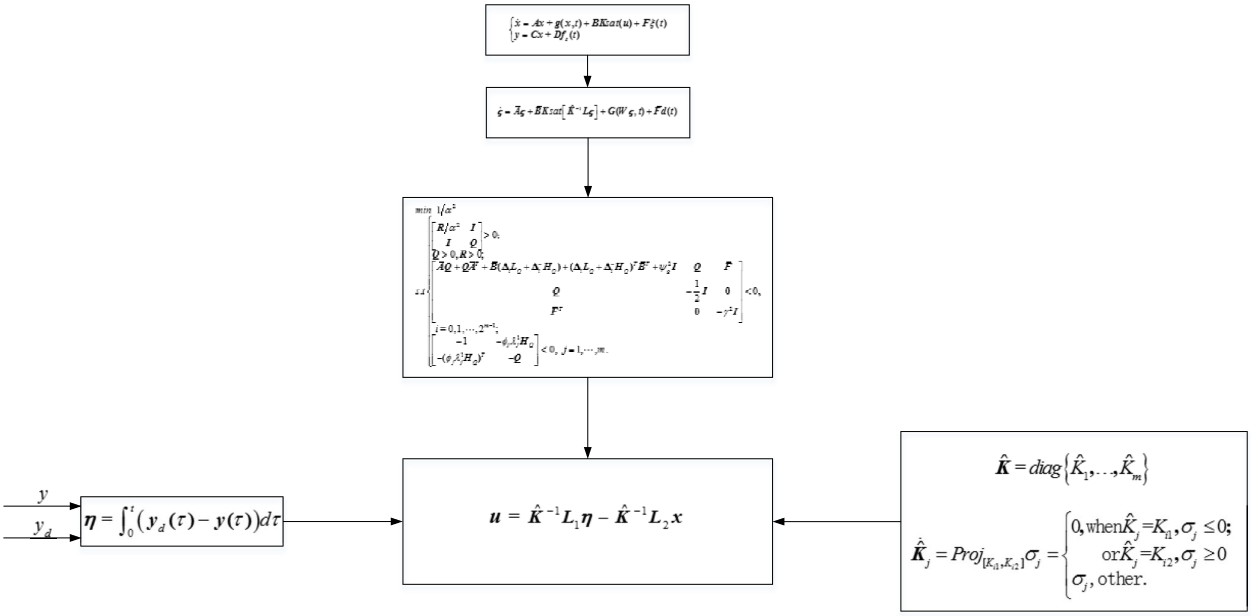

FIGURE 2. **The design flow chart of proposed controller.**

Definition 1: $\boldsymbol{\Delta}$ are the diagonal matrices with m row and m column, and the item of diagonal line is one or zero, obviously, 2^m elements are contained in the matrices $\boldsymbol{\Delta}$, define the ith matrix as Δ_i, and $i \in \aleph\{0, \cdots, 2^m-1\}$,we can find $i = z_1 2^{m-1}+z_2 2^{m-2}+\cdots+z_m$, where $z_j \in \{0, 1\}$, in this case, the elements of diagonal line are $\{1-z_1, 1-z_2, \cdots, 1-z_m\}$, define $\boldsymbol{\Delta}_i^- = \boldsymbol{I}_{m\times m} - \boldsymbol{\Delta}_i$, it is obviously that $\boldsymbol{\Delta}_i^- \in \boldsymbol{\Delta}$.

In order to illustrate the definition 1, we can take the case $m = 2$ as an example to illustrate it. When the case $i = 0$ is correct, then we can find $z_1 = 0$, $z_2 = 0$ and $\boldsymbol{\Delta}_0 = \begin{bmatrix} 1 & 0 \\ 0 & 1 \end{bmatrix}$. When the case $i = 1$ is correct, then we can find $z_1 = 0$, $z_2 = 1$ and $\boldsymbol{\Delta}_1 = \begin{bmatrix} 1 & 0 \\ 0 & 0 \end{bmatrix}$.

Under the above description, Lemma 1 related with saturation is proposed as follows.

Lemma 1: For the given matrices $\boldsymbol{G}, \boldsymbol{H} \in \boldsymbol{R}^{m\times n}$, if $\boldsymbol{x} \in \Xi(\boldsymbol{H})$ is satisfied, then $sat(\boldsymbol{Gx}) \in co \left\{\boldsymbol{\Delta}_i\boldsymbol{Gx} + \boldsymbol{\Delta}_i^-\boldsymbol{Hx}, i \in [0, 2^m-1]\right\}$ is also satisfied, where co is the convex description. Under this assumption, there are η_i, where $\eta_i \geq 0$, $i \in [0, 2^m-1]$, and satisfy $\sum_{i=0}^{2^m-1} \eta_i = 1$, which make the saturation $sat(\boldsymbol{Gx})$ can be described as follows,

$$sat(\boldsymbol{Gx}) = \sum_{i=0}^{2^m-1} \eta_i(\boldsymbol{\Delta}_i\boldsymbol{G} + \boldsymbol{\Delta}_i^-\boldsymbol{H})\boldsymbol{x} \tag{4}$$

We can find in the **Lemma 1,** for the saturated item $sat\ (\boldsymbol{u})$, if the auxiliary matrix $\boldsymbol{H}$ satisfy $\left|\hat{\boldsymbol{K}}^{-1}\boldsymbol{H}\varsigma\right|_j \leq 1$,where $j = 1, \ldots, m$, then the extended system(3) can be transformed as follow,

$$\dot{\varsigma} = \sum_{i=0}^{2^m-1} \eta_i \left(\bar{\boldsymbol{A}} + \bar{\boldsymbol{B}}\boldsymbol{K}\hat{\boldsymbol{K}}^{-1}(\boldsymbol{\Delta}_i\boldsymbol{L} + \boldsymbol{\Delta}_i^-\boldsymbol{H})\right)\varsigma$$
$$+\boldsymbol{G}(\boldsymbol{W}\varsigma, t) + \bar{\boldsymbol{F}}d(\boldsymbol{t}) \tag{5}$$

where $\boldsymbol{\Delta}$ are the diagonal matrices with m row and m column in formula (5), and the matrix $\boldsymbol{\Delta}_i$ and $\boldsymbol{\Delta}_i^-$ can be obtained through the description shown in definition 1, η_i shown in formula (5) can be obtained through the following formula (6).

$$\eta_i = \prod_{j=1}^{m}\left[z_j(1-\mu_j) + (1-z_j)\mu_j\right] \tag{6}$$

where $i = z_1 2^{m-1} + z_2 2^{m-2} + \cdots + z_m$,

$$\mu_j = \begin{cases} 1, & \textbf{when } \lambda_j^1\boldsymbol{L}\varsigma = \lambda_j^1\boldsymbol{H}\varsigma \\ \dfrac{sat\left[\hat{\boldsymbol{K}}_j^{-1}\lambda_j^1\boldsymbol{L}\varsigma\right] - \hat{\boldsymbol{K}}_j^{-1}\lambda_j^1\boldsymbol{H}\varsigma}{\hat{\boldsymbol{K}}_j^{-1}\lambda_j^1\boldsymbol{L}\varsigma - \hat{\boldsymbol{K}}_j^{-1}\lambda_j^1\boldsymbol{H}\varsigma}, & other. \end{cases}$$

Besides, the adaptive estimation law $\hat{\boldsymbol{K}} = diag\left\{\hat{K}_1, \ldots, \hat{K}_m\right\}$ is shown as follows,

$$\dot{\hat{\boldsymbol{K}}}_j = Proj_{[K_{i1},K_{i2}]}\sigma_j = \begin{cases} 0, & \text{when } \hat{K}_j = K_{i1}, \sigma_j \leq 0; \\ \text{or } \hat{K}_j = K_{i2}, & \sigma_j \geq 0 \\ \sigma_j, & \text{others.} \end{cases} \tag{7}$$

where *Proj* stands for project law, which can make the fault estimation $\hat{\boldsymbol{K}}_j$ project to the range $[K_{i1}, K_{i2}]$. σ_j is shown as follows,

$$\sigma_j = \rho_j\hat{\boldsymbol{K}}_j^{-1}\varsigma^T\boldsymbol{P}\bar{\boldsymbol{B}}_j\lambda_j^1\sum_{i=0}^{2^m-1}\eta_i(\Delta_i\boldsymbol{F} + \Delta_i^-\boldsymbol{H})\varsigma \tag{8}$$

where σ_j represent the adaptive controller gain designed, ρ_j stands for adaptive gain constant, the matrix $\bar{\boldsymbol{B}}$ is shown as

$\bar{\boldsymbol{B}} = [b_1, \cdots, b_m]$, and $\bar{\boldsymbol{B}}_j = \left[0, \cdots, b_j, \cdots, 0\right]$, λ_j^1 is a row vector where the jth value is one, and the other is zero. Meanwhile, define the matrix $\tilde{\boldsymbol{K}} = \hat{\boldsymbol{K}} - \boldsymbol{K} = diag\left\{\tilde{K}_1, \cdots, \tilde{K}_m\right\}$, as the $\boldsymbol{i}$ th fault value $\boldsymbol{K}_i$ is unknown, so we can get the conclusion $\dot{\hat{\boldsymbol{K}}}_j = \dot{\tilde{\boldsymbol{K}}}_j$.

Considering the constraints $\left|\hat{\boldsymbol{K}}^{-1}\boldsymbol{H}\varsigma\right|_j \le 1$, and define the new matrix $\bar{\boldsymbol{H}} = \hat{\boldsymbol{K}}^{-1}\boldsymbol{H}$, then we can obtain a linear polyhedron invariant set of several, the detailed mathematical description is shown as follows,

$$\Xi\left(\bar{\boldsymbol{H}}_j\right) = \left\{\varsigma \in \boldsymbol{R}^{n+p} \,\middle|\, \left|(\bar{\boldsymbol{H}}_j)\varsigma\right| \le 1, j = 1, \cdots m\right\} \tag{9}$$

Define a positive definite matrix $\boldsymbol{P} \in R^{(n+p)\times(n+p)}$, and a new invariant set $\Omega\left(\boldsymbol{P}, 1\right)$, the detailed information of $\Omega\left(\boldsymbol{P}, 1\right)$ is shown as follows,

$$\Omega\left(\boldsymbol{P}, 1\right) = \left\{\varsigma \in \boldsymbol{R}^{n+p} \,\middle|\, \varsigma^T\boldsymbol{P}\varsigma + \sum_{j=1}^{m}\frac{\tilde{\boldsymbol{K}}_j^2}{\rho_j} \le 1, \boldsymbol{P} = \boldsymbol{P}^T > 0\right\} \tag{10}$$

For the extended system(5), the goal of active fault tolerant control design is shown in the following. Designing the gain matrices $\boldsymbol{L}, \boldsymbol{H}$ and adaptive law $\hat{\boldsymbol{K}}$, make sure the original system asymptotically stable, meanwhile, the system output can track the given value $\boldsymbol{y}_d$ under multiple faults existing. So the following issue is to provide the detailed design method for gain matrix $\boldsymbol{L}$ and $\boldsymbol{H}$, and the detailed information are shown in part 4.

IV. THE CALCULATING ALGORITHM OF CONTROLLER WITH LINEAR MATRIX INEQUALITY

Theorem 1: If there are positive define matrix $\boldsymbol{Q} \in \boldsymbol{R}^{(n+p)\times(n+p)}$, feasible matrix $\boldsymbol{L}_Q \in \boldsymbol{R}^{m\times(n+p)}$ and $\boldsymbol{H}_Q \in \boldsymbol{R}^{m\times(n+p)}$, given positive constant γ, the following linear matrix inequality exists, (11) and (12), as shown at the bottom of the next page, meanwhile, the adaptive law $\hat{\boldsymbol{K}}$ is calculated as (7) and (8), then the closed loop system (5) is asymptotic stable, and the system matrix is shown as $\boldsymbol{P} = \boldsymbol{Q}^{-1}, \boldsymbol{L} = \boldsymbol{L}_Q\boldsymbol{P}, \boldsymbol{H} = \boldsymbol{H}_Q\boldsymbol{P}$.

Prove,define as $\Gamma = \dot{V} + \varsigma^T\varsigma - \gamma^2\boldsymbol{d}^T\boldsymbol{d}$, while $V(t)$ is shown as $V(t) = \varsigma^T\boldsymbol{P}\varsigma + \sum_{j=1}^{m}\frac{\tilde{K}_j^2}{\rho_j}$, while $V(t) = \varsigma^T\boldsymbol{P}\varsigma + \sum_{j=1}^{m}\frac{\tilde{K}_j^2}{\rho_j}$,as $\Omega\left(\boldsymbol{P}, 1\right) \subset \Xi\left(\bar{\boldsymbol{H}}_j\right)$, the derivative of $V(t)$ is shown as follows,

$$\dot{V}(t) = 2\varsigma^T\boldsymbol{P}\left[\begin{array}{l}\sum_{i=0}^{2^m-1}\eta_i\left(\bar{A} + \boldsymbol{B}\bar{K}\hat{K}^{-1}(\boldsymbol{\Delta}_i\boldsymbol{L} + \boldsymbol{\Delta}_i^-\boldsymbol{H})\right)\varsigma \\ +\boldsymbol{G}(w\varsigma, t) + \bar{\boldsymbol{F}}d(t)\end{array}\right] + 2\sum_{j=1}^{m}\frac{\tilde{K}_j\dot{\hat{K}}_j}{\rho_j} \tag{13}$$

As $\boldsymbol{K}\hat{\boldsymbol{K}}^{-1} = \boldsymbol{I}_m - \tilde{\boldsymbol{K}}\hat{\boldsymbol{K}}^{-1}$, then the conclusion shown in formula (13) can be transformed as follows,

$$\begin{aligned}\dot{V}(t) &= 2\varsigma^T\boldsymbol{P}\left[\begin{array}{l}\sum_{i=0}^{2^m-1}\eta_i\left(\bar{\boldsymbol{A}} + \bar{\boldsymbol{B}}(\boldsymbol{I}_m - \tilde{\boldsymbol{K}}\hat{\boldsymbol{K}}^{-1})(\boldsymbol{\Delta}_i\boldsymbol{L} + \boldsymbol{\Delta}_i^-\boldsymbol{H})\right)\varsigma \\ +\boldsymbol{G}(w\varsigma, t)\end{array}\right] \\ &\quad + 2\varsigma^T\boldsymbol{P}\bar{\boldsymbol{F}}d(t) + 2\sum_{j=1}^{m}\frac{\tilde{K}_j\dot{\hat{K}}_j}{\rho_j}\end{aligned} \tag{14}$$

Combining the conclusion of $2\varsigma^T\boldsymbol{P}\boldsymbol{G}(w\varsigma, t) \le \varsigma^T\left(\psi_g^2\boldsymbol{P}^2 + \boldsymbol{I}\right)\varsigma$, then the form shown in (14) can be transformed as follows,

$$\begin{aligned}\dot{V}(t) &\le \varsigma^T\left[\begin{array}{l}2\boldsymbol{P}\bar{\boldsymbol{B}}\sum_{i=1}^{2^m-1}\eta_i(\boldsymbol{\Delta}_i\boldsymbol{L} + \boldsymbol{\Delta}_i^-\boldsymbol{H})\varsigma + \left(\psi_g^2\boldsymbol{P}^2 + \boldsymbol{I}\right) \\ -2\boldsymbol{P}\bar{\boldsymbol{B}}\sum_{i=0}^{2^m-1}\eta_i\tilde{\boldsymbol{K}}\hat{\boldsymbol{K}}^{-1}(\boldsymbol{D}_i\boldsymbol{F} + \boldsymbol{D}_i^-\boldsymbol{H}) + \boldsymbol{P}\bar{\boldsymbol{A}} + \bar{\boldsymbol{A}}^T\boldsymbol{P}\end{array}\right]\varsigma \\ &\quad + 2\varsigma^T P\bar{F}d(\boldsymbol{t}) + 2\sum_{j=1}^{m}\frac{\tilde{\boldsymbol{K}}_j\dot{\hat{\boldsymbol{K}}}_j}{\rho_j}\end{aligned} \tag{15}$$

Combining the adaptive law of $\dot{\hat{\boldsymbol{K}}}_j$ and conclusion shown in (7)(8), then we can obtain,

$$\dot{V}(t) \le \varsigma^T\left[\begin{array}{l}\boldsymbol{P}\bar{\boldsymbol{A}} + \bar{\boldsymbol{A}}^T\boldsymbol{P} + \psi_g^2\boldsymbol{P}^2 + \boldsymbol{I} \\ +2\boldsymbol{P}\bar{\boldsymbol{B}}\sum_{i=0}^{2^m-1}\eta_i(\boldsymbol{\Delta}_i\boldsymbol{L} + \boldsymbol{\Delta}_i^-\boldsymbol{H})\varsigma\end{array}\right]\varsigma + 2\varsigma^T\boldsymbol{P}\bar{\boldsymbol{F}}d(\boldsymbol{t}) \tag{16}$$

For the given value γ, if the inequality of $\|\varsigma\|_2 < \gamma\left\|\boldsymbol{d}(\boldsymbol{t}))\right\|_2$ is satisfied, then we can obtain the following formula,

$$\Gamma \le \varsigma^T\left[\begin{array}{l}\boldsymbol{P}\bar{\boldsymbol{A}} + \bar{\boldsymbol{A}}^T\boldsymbol{P} + \psi_g^2\boldsymbol{P}^2 + \boldsymbol{I} \\ +2\boldsymbol{P}\bar{\boldsymbol{B}}\sum_{i=1}^{2^m-1}\eta_i(\boldsymbol{\Delta}_i\boldsymbol{L} + \boldsymbol{\Delta}_i^-\boldsymbol{H})\end{array}\right]\varsigma + 2\varsigma^T\boldsymbol{P}\bar{\boldsymbol{F}}d(t) + \varsigma^T\varsigma - \gamma^2\boldsymbol{d}^T\boldsymbol{d} \tag{17}$$

Further more, the above formula (17) can be transformed as follows,

$$\Gamma \le \left[\varsigma^T\ \boldsymbol{d}^T(t)\right]\left[\begin{array}{cc}\begin{array}{l}2\boldsymbol{P}\bar{\boldsymbol{B}}\sum_{i=1}^{2^m-1}\eta_i(\boldsymbol{\Delta}_i\boldsymbol{L} + \boldsymbol{\Delta}_i^-\boldsymbol{H}) \\ +\psi_g^2\boldsymbol{P}^2 + 2\boldsymbol{I} + \boldsymbol{P}\bar{\boldsymbol{A}} + \bar{\boldsymbol{A}}^T\boldsymbol{P}\end{array} & \boldsymbol{P}\bar{\boldsymbol{F}} \\ (\boldsymbol{P}\bar{\boldsymbol{F}})^T & -\gamma^2\boldsymbol{I}\end{array}\right] \times \left[\begin{array}{c}\varsigma \\ \boldsymbol{d}(t)\end{array}\right] \tag{18}$$

According to the conclusion shown in (18), define $\boldsymbol{\Theta} = \left[\begin{array}{cc}\begin{array}{l}2\boldsymbol{P}\bar{\boldsymbol{B}}\sum_{i=1}^{2^m-1}\eta_i(\boldsymbol{\Delta}_i\boldsymbol{L} + \boldsymbol{\Delta}_i^-\boldsymbol{H}) + \psi_g^2\boldsymbol{P}^2 + 2\boldsymbol{I} \\ +\boldsymbol{P}\bar{\boldsymbol{A}} + \bar{\boldsymbol{A}}^T\boldsymbol{P}\end{array} & \boldsymbol{P}\bar{\boldsymbol{F}} \\ (\boldsymbol{P}\bar{\boldsymbol{F}})^T & -\gamma^2\boldsymbol{I}\end{array}\right]$, Suppose $\boldsymbol{\Theta} < 0$, then combining the conclusion provided in the lemma of Schur, and the conclusion can be obtained shown in (11).

In order to make the control input in the range of $\Xi\left(\bar{\boldsymbol{H}}_j\right)$, in other words, for any given extended state $\boldsymbol{\varsigma}$, define $\Omega_0(\boldsymbol{P},1) = \left\{\boldsymbol{\varsigma} \in \boldsymbol{R}^{n+p}; \boldsymbol{\varsigma}^T\boldsymbol{P}\boldsymbol{\varsigma} \le 1\right\}$, and we can find that $\Omega(\boldsymbol{P},1) \subset \Omega_0(\boldsymbol{P},1)$, so as long as the form $\Omega_0(\boldsymbol{P},1) \subset \Xi\left(\bar{\boldsymbol{H}}_j\right)$ exist, so only if the following formula exists,

$$\begin{bmatrix} 1 & (\hat{\boldsymbol{K}}^{-1})_j\boldsymbol{H}_Q \\ \boldsymbol{H}_Q^T(\hat{\boldsymbol{K}}^{-1})_j^T & \boldsymbol{Q}\end{bmatrix} > 0, j = 1,\cdots,m \tag{19}$$

For the adaptive law $\hat{\boldsymbol{K}}^{-1}$, we can define a set related with it, the detailed information is shown in (20),

$$\Upsilon \overset{def}{=} \left\{\begin{matrix}\Theta^i \left|\Theta^i = diag\left\{\phi_1,\cdots,\phi_m\right\}, \phi_j = \boldsymbol{K}_j^{-1},\right. \\ i = 0,1,\cdots,2^{m-1}, j = 1,\cdots,m\end{matrix}\right\} \tag{20}$$

As the set of Υ satisfy the characteristic of convex, so there are $\beta_i \ge 0$, the equation of $\sum_{i=0}^{2^m-1}\beta_i = 1$ exists, and the adaptive law $\hat{\boldsymbol{K}}^{-1}$ can be expressed as $\hat{\boldsymbol{K}}^{-1} = \sum_{i=0}^{2^m-1}\beta_i\Theta^i$, thus the jth column of $\hat{\boldsymbol{K}}^{-1}$ is described as $(\hat{\boldsymbol{K}}^{-1})_j = \sum_{i=0}^{2^m-1}\beta_i(\Theta^i)_j = \sum_{i=0}^{2^m-1}\beta_i\phi_j\lambda_j^1$, and then the form of (19) can be described as follows,

$$\begin{bmatrix} 1 & (\sum_{i=0}^{2^m-1}\beta_i\phi_j\lambda_j^1)_j\boldsymbol{H}_Q \\ \boldsymbol{H}_Q^T(\sum_{i=0}^{2^m-1}\beta_i\phi_j\lambda_j^1)_j^T & \boldsymbol{Q}\end{bmatrix} = \sum_{i=0}^{2^m-1}\beta_i\begin{bmatrix} 1 & \phi_j\lambda_j^1\boldsymbol{H}_Q \\ (\phi_j\lambda_j^1\boldsymbol{H}_Q)^T & \boldsymbol{Q}\end{bmatrix} > 0, j = 1,\cdots,m \tag{21}$$

Analysis the conclusion shown in (21), and the constraints of (12) can be obtained.

From the above analysis, we can find, through designing the fault tolerant controller, the extended system is asymptotic stable in the invariant set of $\Omega(\boldsymbol{P},1)$, and the invariant set can be described as fault tolerant attraction region. One goal of fault tolerant control design is to maximize the attraction region, in order to realize the objective, first we define the new invariant set X_R which is described as $X_R = \left\{\varsigma \in \boldsymbol{R}^{n+p}; \varsigma^T\boldsymbol{R}\varsigma \le 1\right\}$, we can maximize the attraction region of fault tolerant control, and obtain the best control performance. Then, to obtain the solve of (11) and(12), the following optimization problem can be obtained through convex optimization,

$$\begin{aligned} & min 1\big/\alpha^2 \\ & s.t \begin{cases} \begin{bmatrix} \boldsymbol{R}\big/\alpha^2 & \boldsymbol{I} \\ \boldsymbol{I} & \boldsymbol{Q}\end{bmatrix} > 0; \\ Q > 0, R > 0; \\ formula(11)(12). \end{cases}\end{aligned} \tag{22}$$

where $\boldsymbol{R}$ is the chosen positive definite matrix. From the prove process of **Theorem1**, we can find, for the extended system (5), combining the convex description of nonlinearity, designing the adaptive law shown as (7) and (8), and the fault tolerant controller as (22), and then we can get the gain $\boldsymbol{L}$ *as* $\boldsymbol{L} = \boldsymbol{L}_Q\boldsymbol{P}$, then the extended system will be asymptotic stable in the invariable set $\Omega(\boldsymbol{P},1)$ and obtain the satisfied fault tolerant control performance.

Remark 4: The relational parameters in the fault tolerant controller contain the matrices $\boldsymbol{P}, \boldsymbol{H}, \boldsymbol{L}$. First by solving the optimization problem shown in formula(22), the matrices $\boldsymbol{Q}, \boldsymbol{L}_{\boldsymbol{Q}}, \boldsymbol{H}_{\boldsymbol{Q}}$ can be received, then, the matrices $\boldsymbol{P}, \boldsymbol{H}, \boldsymbol{L}$ can be gotten. Besides, the parameter ρ_j is chosen according to the specific case, in common between 0 and 1.

V. NUMERICAL EXAMPLE

In order to illustrate the effectiveness of proposed method proposed in this paper, we take the model of multi-effector aircraft with wing canard presented in paper [28] as an example, the simulation will be carried on. Firstly, linearization and reduced order dealing will be taken, when the state value of plane is shown as $H = 3000m$, $Ma = 0.22$, and we can obtain the system state model which can be described as (1), while $\boldsymbol{x}$ stands for $\boldsymbol{x} = [\alpha\beta pqr]^T$, where α, β, p, q, r represents for angle of attack, angle of sideslip, roll rate, pitching angle rate and yaw angle rate respectively. The control inputs are described as $\boldsymbol{u} = [\delta_c\ \delta_{re}\ \delta_{le}\ \delta_r]^T$, and δ_c, δ_{re}, δ_{le}, δ_r stands for wing canard, right elevon, left elevon, and rudder control inputs, the detailed system matrices are shown as

$$\begin{bmatrix} \bar{A}Q + Q\bar{A}^T + \bar{\boldsymbol{B}}(\boldsymbol{\Delta}_i\boldsymbol{L}_Q + \boldsymbol{\Delta}_i^-\boldsymbol{H}_Q) + (\boldsymbol{\Delta}_i\boldsymbol{L}_Q + \boldsymbol{\Delta}_i^-\boldsymbol{H}_Q)^T\bar{\boldsymbol{B}}^T + \psi_g^2\boldsymbol{I} & \boldsymbol{Q} & \bar{\boldsymbol{F}} \\ \boldsymbol{Q} & -\frac{1}{2}\boldsymbol{I} & \boldsymbol{0} \\ \bar{\boldsymbol{F}}^T & \boldsymbol{0} & -\gamma^2\boldsymbol{I}\end{bmatrix} < 0;$$

$$\boldsymbol{i = 0, 1, \cdots, 2^{m-1}} \tag{11}$$

$$\begin{bmatrix} -1 & -\phi_j\lambda_j^1\boldsymbol{H}_Q \\ -(\phi_j\lambda_j^1\boldsymbol{H}_Q)^T & -\boldsymbol{Q}\end{bmatrix} < 0, j = 1,\cdots,m \tag{12}$$

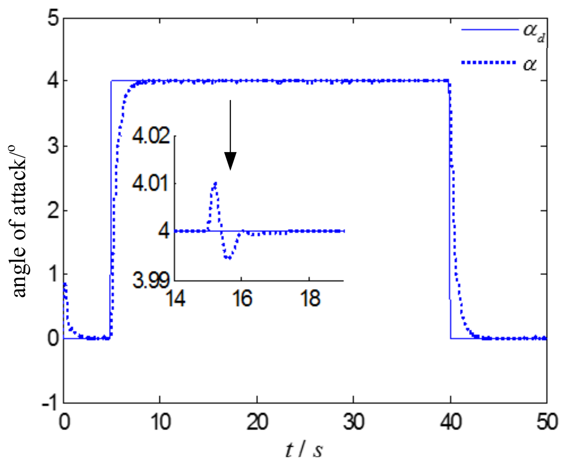

FIGURE 3. The angle of attack response of the fault tolerant controller.

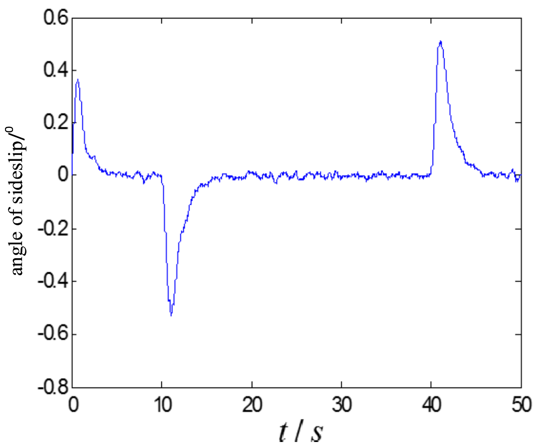

FIGURE 4. Angle of sideslip response of the fault tolerant controller.

follows,

$$\boldsymbol{A} = \begin{bmatrix} -0.5432 & 0.0137 & 0 & 0.9778 & 0 \\ 0 & -0.1179 & 0.2215 & 0 & -0.9661 \\ 0 & -10.5128 & -0.9967 & 0 & 0.6176 \\ 2.6221 & -0.0030 & 0 & -0.5057 & 0 \\ 0 & 0.7075 & -0.0939 & 0 & -0.2127 \end{bmatrix},$$

$$\mathbf{B} = \begin{bmatrix} 0.0069 & -0.0866 & -0.0866 & 0.0004 \\ 0 & 0.0119 & -0.0119 & 0.0287 \\ 0 & -4.2423 & 4.2423 & 1.4871 \\ 1.6532 & -1.2735 & -1.2735 & 0.0024 \\ 0 & -0.2805 & 0.2805 & -0.8823 \end{bmatrix},$$

$$\boldsymbol{C} = \begin{bmatrix} 1 & 0 & 0 & 0 & 0 \\ 0 & 1 & 0 & 0 & 0 \\ 0 & 0 & 1 & 0 & 0 \end{bmatrix}$$

Besides, the disturbances matrix $\boldsymbol{F}$ is five identity matrix, the upper bounds of actuators deflecting are described as $\delta_c \in [-55°, 25°]$, $\delta_{re} \in [-30°, 30°]$, $\delta_{le} \in [-30°, 30°]$, $\delta_r \in [-30°, 30°]$. The reference output is designed as $\boldsymbol{r}(t) = [\alpha, \beta, p]$,and the command output $\alpha(t)$ is described

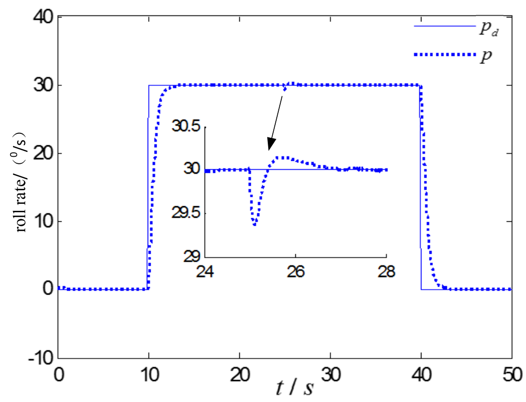

FIGURE 5. Roll rate response of the fault tolerant controller.

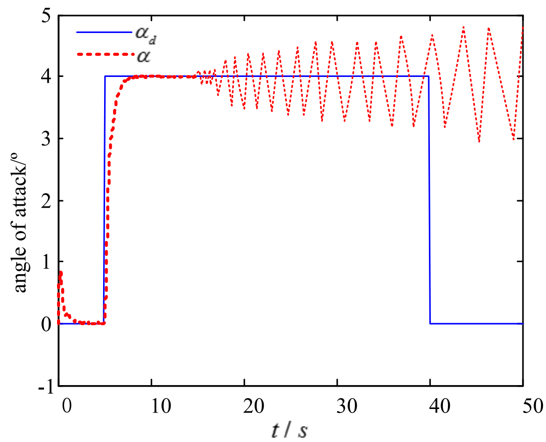

FIGURE 6. The angle of attack response of PI controller.

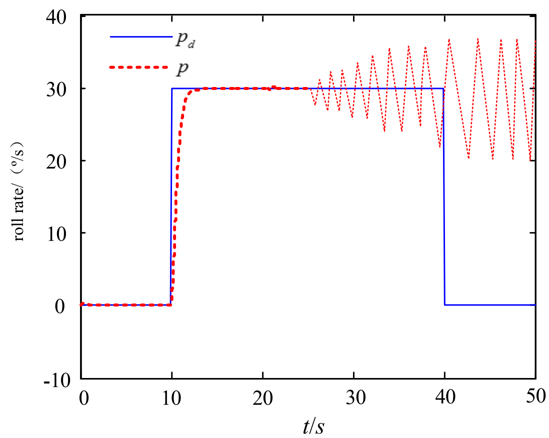

FIGURE 7. The roll rate response of PI controller.

as $\alpha_d = \begin{cases} 0°, t < 5\text{s} \\ 4°, 5 \le t < 40\text{s} \\ 0°, t \ge 40\text{s} \end{cases}$, the command output $\beta(t)$ is described as 0, the command output $p(t)$ is described as $p_d = \begin{cases} 0°/s, t < 10\text{s} \\ 30°/s, 10 \le t < 40\text{s} \\ 0°/s, t \ge 40\text{s} \end{cases}$. Suppose the disturbances are the Gaussian white noise with amplitude of 1, for the above

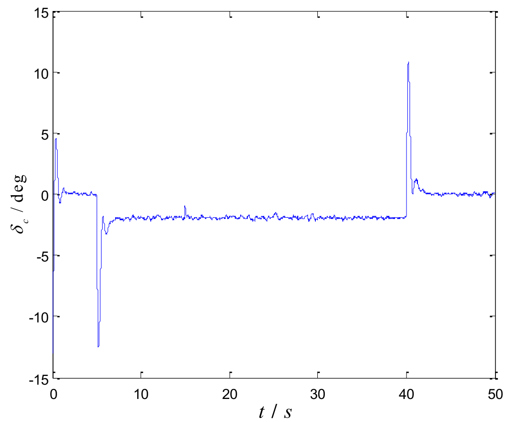

FIGURE 8. Wing canard of the fault tolerant controller.

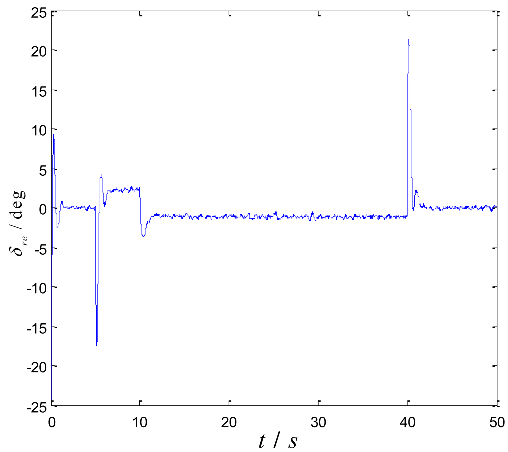

FIGURE 9. Right elevon of the fault tolerant controller.

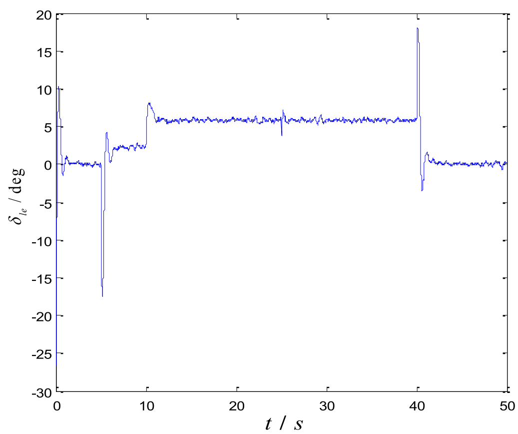

FIGURE 10. Left elevon of the fault tolerant controller.

plane model, we suppose the wing canard actuating efficiency reduce 50% at the time of 15 second, besides, the left elevon actuating efficiency reduce 40% at the time of 25 second, according to the conclusion shown in (11)(12), combining the tools of linear matrix inequality in Matlab, we can obtain the parameter and matrices of integrated active fault tolerant controller, the detailed information are shown in the equation at the bottom of the next page.

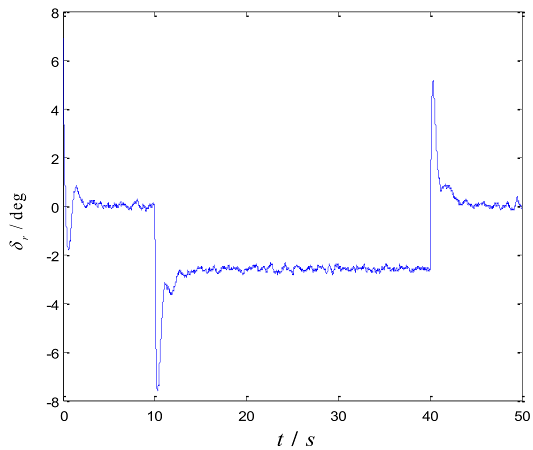

FIGURE 11. Rudder of the fault tolerant controller.

Through the above system design and analysis, we can obtain angle of attack, sideslip angle, roll angle response curves, and they are shown in fig3,4,5. Analyzing the angle of attack response which has been shown in fig3, we can find when the wing canard lose the actuating efficiency partly, in the beginning, the angle of attack will wave in short time, and the wave amplitude is less than 0.01°, then, it will return to command output of 4° in less than one second. Similarly, through analyzing the results shown in fig4, we can find when the left elevon actuating efficiency reduce partly at the time of 25 second, the roll rate will wave in short time and return to the command value in less than 2 seconds. Combing the analysis of simulation results shown in fig3,4,5. We can find when the actuators of airplane emerge partly efficiency loss, through designing the integrated active fault tolerant controller, the attitude angle and angle rate will track to the command output, meanwhile, we can find, the noises and disturbances will not affect the system output, and these show the controller will have good robust performance.

In order to illustrate the effectiveness of fault tolerance controller proposed in this paper, the comparison will be carried on between the fault tolerance controller and PID controller. The angle of attack response of PID controller is shown in Fig.6, We can find, when the wing canard actuator work normally, under the reaction of PID controller, the angle of attack can reach to the command value, but when the wing canard actuator break in the 15 second, the angle of attack can not maintain in the command value, and occur chattering. This shows the PID controller for the aircraft can not realize satisfied results. Fig.7 shows the roll rate response of PI controller. It is obvious that the roll rate does not reach to the command value when faults takes place, and the command control results can not be realized in the PID controller.

Besides, through simulation, we obtain the actuator response, the wing canard, right elevon, left elevon and rudder actuator angle response are shown in Fig8-11. Through analyzing the results shown in Fig8-11, we can find the actuator response will be in saturated range, and the actuator response is suitable for actual characteristic, these results show the

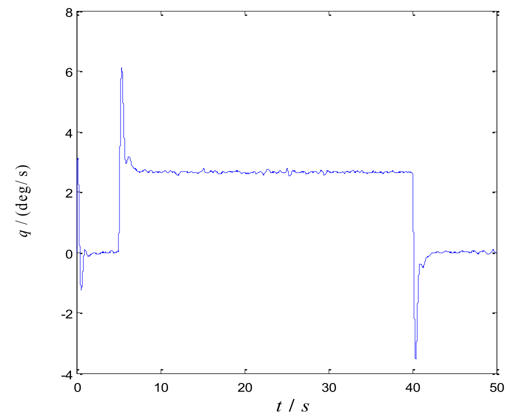

FIGURE 12. Pitch angle rate response of the fault tolerant controller.

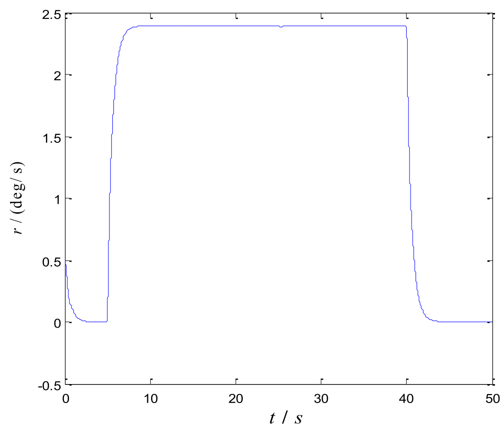

FIGURE 13. Yaw angle rate response of the fault tolerant controller.

integrated fault tolerant controller presented in this paper can realize satisfied control results.

Meanwhile, through the simulation, we can obtain the pitch angle and yaw angle rate response shown in Fig12 and Fig13. Analyzing the results shown in Fig12 and Fig13, we can find, when the wing canard and left elevon faults of efficiency loss occur, the pitch angle and yaw angle rate will return to normal response under the fault tolerant controller.

In the foregoing description, the little fault type of actuator efficiency reducing is considered, next a serious fault type

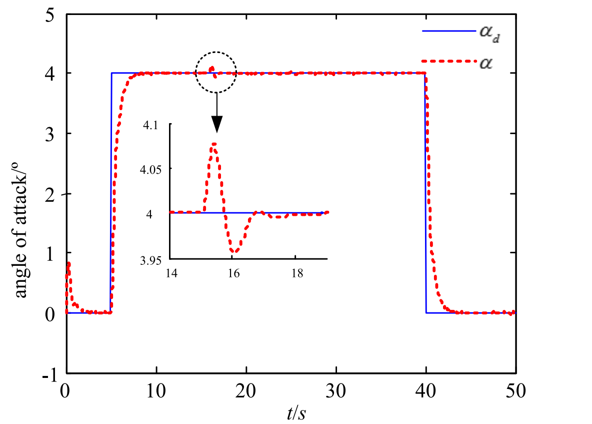

FIGURE 14. The angle of attack response of the fault tolerant controller under serious fault.

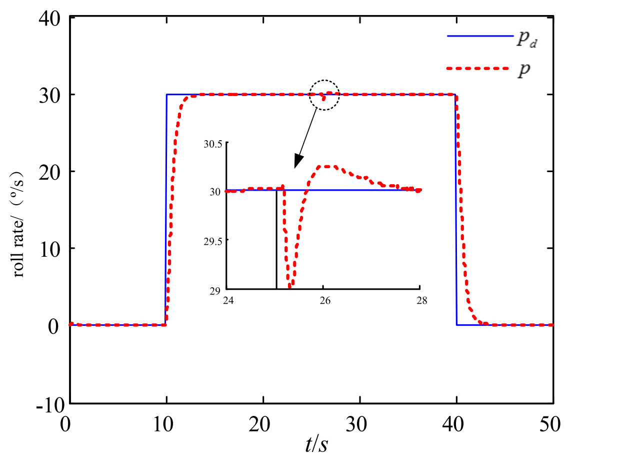

FIGURE 15. The roll rate response of the fault tolerant controller under serious fault.

will be provided to demonstrate the effectiveness of fault tolerant controller. we suppose the wing canard actuating efficiency reduce 80% at the time of 15 second, and the left elevon actuating efficiency reduce 60% at the time of 25 second, in this case, the angle of attack and roll rate responses are shown in Fig. 14,15. Analyzing the results shown in Fig14 and Fig15, we can find, when the wing canard and left elevon serious faults of efficiency loss occur, the

$$\boldsymbol{L} = \begin{bmatrix} 15.81 & 0 & 0 & -1.02 & 0 & -26.16 & 0.01 & 0 \\ 31.22 & -4.62 & 0.55 & -0.16 & 1.02 & -51.04 & 3.79 & -1.47 \\ 31.22 & 4.60 & -0.55 & -0.16 & -1.01 & -51.04 & -3.72 & 1.46 \\ 0 & -17.41 & -0.13 & 0 & 3.88 & 0 & 15.73 & -1.95 \end{bmatrix}$$

$$\boldsymbol{P} = \begin{bmatrix} 0.11 & 0 & 0 & 0 & 0 & -0.17 & 0 & 0 \\ 0 & 8.67 & 0.03 & 0 & 0.05 & 0 & -7.73 & 1.11 \\ 0 & 0.03 & 0.11 & 0 & 0 & 0 & -0.04 & -0.17 \\ 0 & 0 & 0 & 0.11 & 0 & 0 & 0 & 0 \\ 0 & 0.05 & 0 & 0 & 0.06 & 0 & -0.04 & 0 \\ -0.17 & 0 & 0 & 0 & 0 & 3.51 & 0 & 0 \\ 0 & -7.73 & -0.04 & 0 & -0.04 & 0 & 10.08 & -0.69 \\ 0 & 1.11 & -0.17 & 0 & 0 & 0 & -0.69 & 3.71 \end{bmatrix}.$$

pitch angle and yaw angle rate will return to normal response under the fault tolerant controller, and these demonstrates, even when the challenging scenarios of serious faults occur, the fault tolerant controller proposed in this paper can achieve statisfied control results.

VI. CONCLUSION

The active fault tolerant controller is proposed in this paper, which is used for the system with actuator saturation and multiple faults. Firstly, taking the sensor faults as one part of extended vector, and the original system is transformed to the nonlinear system with multiple actuator faults, and it will simply the controller design procedure. Then, to the deal with the saturation, the items of convex group description are absorbed in the controller design, and these will make sure the control input avoid saturation, besides, the integrated fault tolerant controller with adaptive faults estimate is proposed, and the calculating algorithm of controller is proposed through linear matrix inequality. Finally, a numerical example is proposed to validate the effectiveness of the method presented in this paper. Here we only solve the fault-tolerant control of nonlinear system with saturation and multiple faults. Many issues have not been considered, such as when the nonlinear item $\boldsymbol{g}(\boldsymbol{x},t)$ does not satisfy global *Lipschitz* condition, how to build the controller, etc. These will be our future research directions.

ACKNOWLEDGMENT

The author would like to thank the anonymous reviewers and the associate editor for their helpful remarks, which improved the quality of this article.

REFERENCES

[1] N. Wang and Z. Deng, "Finite-time fault estimator based fault-tolerance control for a surface vehicle with input saturations," *IEEE Trans. Ind. Informat.*, vol. 16, no. 2, pp. 1172–1181, Feb. 2020.
[2] Z. Yu, Z. Liu, Y. Zhang, Y. Qu, and C.-Y. Su, "Distributed finite-time fault-tolerant containment control for multiple unmanned aerial vehicles," *IEEE Trans. Neural Netw. Learn. Syst.*, vol. 31, no. 6, pp. 2077–2091, Jun. 2020.
[3] X. Shao, Q. Hu, Y. Shi, and B. Jiang, "Fault-tolerant prescribed performance attitude tracking control for spacecraft under input saturation," *IEEE Trans. Control Syst. Technol.*, vol. 28, no. 2, pp. 574–582, Mar. 2020.
[4] Y. Li and W. Li, "Research on satisfactory integrated design of event-triggered fault accommodation and network communication saving for NCSs with actuator saturation under non-uniform transmission," *IEEE Access*, vol. 8, pp. 70293–70305, 2020.
[5] L. Sun, "Adaptive fault-tolerant constrained control of cooperative spacecraft rendezvous and docking," *IEEE Trans. Ind. Electron.*, vol. 67, no. 4, pp. 3107–3115, Apr. 2020.
[6] N. Zhou, Y. Kawano, and M. Cao, "Neural network-based adaptive control for spacecraft under actuator failures and input saturations," *IEEE Trans. Neural Netw. Learn. Syst.*, vol. 31, no. 9, pp. 3696–3710, Sep. 2020.
[7] H. Başak, E. Kemer, and E. Prempain, "A passive fault-tolerant switched control approach for linear multivariable systems: Application to a quadcopter unmanned aerial vehicle model," *J. Dyn. Syst., Meas., Control*, vol. 142, no. 3, pp. 1–8, Mar. 2020.
[8] J. Li, Y. Ma, and L. Fu, "Fault-tolerant passive synchronization for complex dynamical networks with Markovian jump based on sampled-data control," *Neurocomputing*, vol. 350, pp. 20–32, Jul. 2019.
[9] B. Wang, Y. Shen, and Y. Zhang, "Active fault-tolerant control for a quadrotor helicopter against actuator faults and model uncertainties," *Aerosp. Sci. Technol.*, vol. 99, Apr. 2020, Art. no. 105745.
[10] W. Gang, "ESO-based terminal sliding mode control for uncertain full-car active suspension systems," *Int. J. Automot. Technol.*, vol. 21, no. 3, pp. 691–702, Jun. 2020.
[11] L. Cong, L. Yinghui, Z. Xihua, and L. Peipei, "The adaptive sliding mode observer for the actuator fault reconstruction of nonlinear system with mismatched uncertainties," *Control Theory Appl.*, vol. 31, no. 4, pp. 431–437, 2014.
[12] L. Cong, L. Ying-Hui, W. Chen, and Y. Guo-Qiang, "Design of the robust adaptive sliding mode observer for multiple fault reconstruction," *Control Decis.*, vol. 31, no. 7, pp. 1219–1224, 2016.
[13] L. Cong and L. Ying-Hui, "Design of high gain observers with sliding m ode for the actuator robust fault detection of nonlinear system," *Syst. Eng. Electron.*, vol. 36, no. 8, pp. 1626–1631, 2014.
[14] L. Cong, L. Ying-Hui, and L. Yongzhi, "Unknown actuator fault reconstruction based on the high order terminal sliding mode observer," *J. Xi'an Jiaotong Univ.*, vol. 49, no. 9, pp. 126–133, 2015.
[15] H. Shi, P. Li, C. Su, Y. Wang, J. Yu, and J. Cao, "Robust constrained model predictive fault-tolerant control for industrial processes with partial actuator failures and interval time-varying delays," *J. Process Control*, vol. 75, pp. 187–203, Mar. 2019.
[16] B. Peng, H. Shi, C. Su, and P. Li, "Robust switched predictive control for multi-phase batch processes with uncertainties and unknown disturbances," *J. Process Control*, vol. 94, pp. 110–124, Oct. 2020.
[17] J. Wu, H. Shi, X. Jiang, C. Su, and P. Li, "Stochastic fuzzy predictive fault-tolerant control for time-delay nonlinear system with actuator fault under a certain probability," *Optim. Control Appl. Methods*, vol. 44, no. 4, pp. 1798–1827, Dec. 2022.
[18] H. Shi, L. Zuo, S. Wang, C. Su, and P. Li, "Stochastic robust predictive fault-tolerant control for discrete systems with actuator faults," *Eng. Res. Exp.*, vol. 5, no. 3, Sep. 2023, Art. no. 035041.
[19] L. Wang, J. Song, R. Zhang, and F. Gao, "Constrained model predictive fault-tolerant control for multi-time-delayed batch processes with disturbances: A Lyapunov-Razumikhin function method," *J. Franklin Inst.*, vol. 358, no. 18, pp. 9483–9509, Dec. 2021.
[20] L. Wang and W. Luo, "Linear quadratic predictive fault-tolerant control for multi-phase batch processes," *IEEE Access*, vol. 7, pp. 33598–33609, 2019.
[21] H. Li, S. Wang, H. Shi, C. Su, and P. Li, "Iterative learning hybrid robust predictive fault-tolerant control for nonlinear batch processes with partial actuator faults," *J. Process Control*, vol. 129, Sep. 2023, Art. no. 103054.
[22] X. Li, Q. Luo, L. Wang, R. Zhang, and F. Gao, "Off-policy reinforcement learning-based novel model-free minmax fault-tolerant tracking control for industrial processes," *J. Process Control*, vol. 115, pp. 145–156, Jul. 2022.
[23] L. Wang and B. Li, "Probability based stochastic iterative learning control for batch processes with actuator faults," *IEEE Access*, vol. 7, pp. 141466–141475, 2019.
[24] L. Wang, L. Sun, and W. Luo, "Robust constrained iterative learning predictive fault-tolerant control of uncertain batch processes," *Sci. China Inf. Sci.*, vol. 62, no. 11, pp. 1–3, Nov. 2019.
[25] S. Wang, H. Li, H. Shi, C. Su, and P. Li, "Robust asynchronous switching fault-tolerant control for multi-phase batch processes with time-varying delay," *IEEE Access*, vol. 9, pp. 69365–69381, 2021.
[26] L. Wang, L. Jia, R. Zhang, and F. Gao, "H_∞ output feedback fault-tolerant control of industrial processes based on zero-sum games and off-policy Q-learning," *Comput. Chem. Eng.*, vol. 17, no. 9, pp. 1–14, 2023.
[27] F. Jinhua, *Actuator Fault-Tolerant Control Against Saturation*, Hunan, National University of Defense Technology, Changsha, China, 2013.
[28] L. Forssell and U. Nilsson, *ADMIRE the Aero-Data Model in a Research Environment Version 4.0, Model Description*, document FOI-R-1624-SE, Swedish Defence Agency, Sweden, 2005, pp. 25–34.

CONG LIU was born in Jiangxi, China, in 1988. He received the B.Sc. degree in electrical engineering and automatic control and the M.Sc. and Ph.D. degrees in control science and engineering from Air Force Engineering University (AFEU), Xi'an, China, in 2009, 2012, and 2016, respectively. He is currently a Lecturer with the Department of Aeronautic Instrument and Electrical, AFEU. His research interests include nonlinear observer design, fault reconstruction, and fault-tolerant control.